Fall 8-28-2022

Healthy Exosomes and their Effects on Diabetic Cardiomyocytes

Miguel A. Garza
The University of Texas Rio Grande Valley, miguel.a.garza07@utrgv.edu

Genaro A. Ramírez-Correa
The University of Texas Rio Grande Valley

Maria Lourdes Garza-Rodríguez
Universidad Autónoma de Nuevo León

Andres J. Medina
The University of Texas Rio Grande Valley

Healthy Exosomes and their Effects on Diabetic Cardiomyocytes

Miguel Garza, Genaro Ramírez-Correa, María de Lourdes Garza-Rodríguez, Andres J Medina

University of Texas Rio Grande Valley School of Medicine Department of Molecular Science.

Abstract. Extracellular Vesicles, and more specifically, exosomes, are essential for effective cell-to-cell communication in a wide variety of tissues. In the last couple of decades, these nanovesicles have been proven to be active participants and regulators in many disease processes; therefore, their therapeutic effects have been widely studied and proven in various cardiovascular diseases both, in vitro and in vivo. Thus, this study aims at assessing the effects of running healthy mice exosomes on cardiomyocyte and cardiac tissue samples obtained from diabetic mice. Here, we successfully extract exosomes from mice plasma and detect their presence through the use of anti-CD9 and anti-CD81 antibodies. Further work includes concentrating exosome presence and utilizing a wider variety of exosome-specific antibodies, as well as exploring techniques for more effective exosome extraction from plasma.

Introduction. Cell-to-cell communication is central in both, the proper functioning of every working tissue in our body, as well as in every pathophysiological process underlying every disease. One of the methods through which cells effectively communicate with each other is using extracellular vesicles (EVs), which are ubiquitous and essential information carriers that transport proteins, lipids, signaling molecules, and nucleic material with high specificity. A specific type of EVs, called exosomes, are nanosized EVs of endosomal origin known to be involved in the regulation of many pathophysiological processes throughout our whole body (Barile & Vassalli, 2017). The importance of these types of EVs has been increasingly proven to be more relevant, being involved directly in the pathophysiology of many disease processes,

including tumorigenesis, inflammation, autoimmune diseases, neurodegenerative processes, and cardiomyopathies (EL Andaloussi et al., 2013). Due to their many crucial roles in regulating disease processes, exosome use as a delivery agent of therapeutic components has increasingly popularized in the last couple of decades, with many clinical trials being conducted in a wide range of diseases. Most specifically, exosome benefits and potential therapeutic uses have been proven to have beneficial effects on different cardiovascular diseases. EVs have proven effective in initiating anti-apoptotic activity in cardiomyocytes, inducing proangiogenic activities, improving cardiac tissue function post-myocardial infarction (MI) in vivo, and scar reduction with improved cardiac function in vivo (Barile et al., 2014). Hence in this study, the focus is to extract exosomes from healthy running mice, with the purpose of culturing diabetic mice cardiomyocytes with healthy exosomes, to then assess cardiomyocyte function changes and compare them to control diabetic mice.

Materials and Methods. A total of 4 experimental mice were subject to a running wheel for a period of 6 weeks, with constant measurement of the number of spins and distance run. Plasma was then isolated from each mouse, as well as from 4 wild-type mice. Plasma extraction worked by ethically sacrificing mice by dislocation after isoflurane anesthesia in an oxygen chamber; the heart was cut from the right atria and blood was collected directly from the thoracic cavity using a tuberculin syringe previously impregnated with sodium citrate anticoagulant. Collected blood was placed on 100µL sodium citrate anticoagulant. Blood sat at room temperature for 30 minutes before centrifuging at 2500g for 15 minutes at 4ºC. Plasma samples only from wild-type mice were then fractioned by size using Izon Automatic Fraction Collector (AFC), dividing each plasma sample into 12 different fractions; PBS was the buffer of choice for fractions. Protein concentration for each fraction was determined using Lowry Protein Assay after lysing each

fraction using 1X RIPA buffer and proteinase inhibitor. After the determination of concentrations, only fractions 10, 11, and 12 were considered for subsequent steps. Western Blot was performed using PVDF transfer membrane using iBlot2 Dry Blotting System; anti-CD9 and anti-CD81 1:1000 was used as primary antibodies incubated overnight at 4°C, and anti-Rabbit IgG HRP-linked 1:2000 as secondary antibody incubated for 1 hour at room temperature. Magic Mark and Sea Blue ladders were utilized. Super signal West Pico PLUS Chemiluminescent substrate was used for revelation. Coomassie Blue and Red Ponceau stains were used for visual examination of gel and PVDF membrane, respectively. In the last trial, samples were concentrated using Eppendorf Vacufage Plus, set at 60°C for 20 minutes to yield a 5x concentration.

Results. In the first trial, there was clear evidence of the presence of sufficient protein based on the Lowry Protein Assay (Tables 1 and 2).

	1	2	3
1000	0.646	0.609	0.631
750	0.535	0.449	0.344
500	0.463	0.412	0.353
250	0.204	0.261	0.249
125	0.155	0.19	0.181
25	0.124	0.112	0.116
5	0.116	0.094	0.096
	1	2	
WT2-1 F1	0.122	0.126	
WT2-1 F2	0.107	0.128	
WT2-1 F3	0.131	0.276	
WT2-1 F4	0.193	0.134	
WT2-1 F5	0.155	0.158	
WT2-1 F6	0.177	0.213	
WT2-1 F7	0.215	0.273	
WT2-1 F8	0.365	0.365	
WT2-1 F9	0.383	0.452	
WT2-1 F10	0.622	0.53	
WT2-1 F11	0.658	0.565	
WT2-1 F12	0.646	0.694	
WT2-2 F1	0.114	0.108	
WT2-2 F2	0.302	0.114	
WT2-2 F3	0.116	0.118	
WT2-2 F4	0.118	0.121	
WT2-2 F5	0.131	0.125	
WT2-2 F6	0.159	0.157	
WT2-2 F7	0.212	0.198	
WT2-2 F8	0.252	0.279	
WT2-2 F9	0.318	0.315	
WT2-2 F10	0.308	0.407	
WT2-2 F11	0.459	0.332	
WT2-2 F12	0.502	0.537	

MG1 F1	0.097	0.1
MG1 F2	0.124	0.132
MG1 F3	0.149	0.154
MG1 F4	0.192	0.198
MG1 F5	0.305	0.299
MG1 F6	0.421	0.382
MG1 F7	0.655	0.832
MG1 F8	0.826	0.677
MG1 F9	0.692	0.895
MG1 F10	0.843	0.991
MG1 F11	1.004	1.029
MG1 F12	1.212	0.946
MG2 F1	0.107	0.11
MG2 F2	0.126	0.119
MG2 F3	0.153	0.142
MG2 F4	0.199	0.181
MG2 F5	0.273	0.278
MG2 F6	0.393	0.388
MG2 F7	0.575	0.515
MG2 F8	0.697	0.658
MG2 F9	0.897	0.797
MG2 F10	0.951	0.836
MG2 F11	0.975	0.76
MG2 F12	0.956	0.948

Tables 1 and 2. *Lowry Protein Assay for the 4 wild-type mice samples. Significant protein concentration was observed on fractions 8 and above, where only 10, 11, and 12 were considered to maximize yield.*

However, when loading into the gel, only 1µL of the sample was used by convention for running the gel, yielding a nearly empty membrane. Thus, on trial 2, the full amount of 65µL of protein concentrate was added to the running solution, yielding clear evidence of the presence of the proteins of interest at 26kDa on Coomassie stain and on WB revelation (Figures 1 - 6).

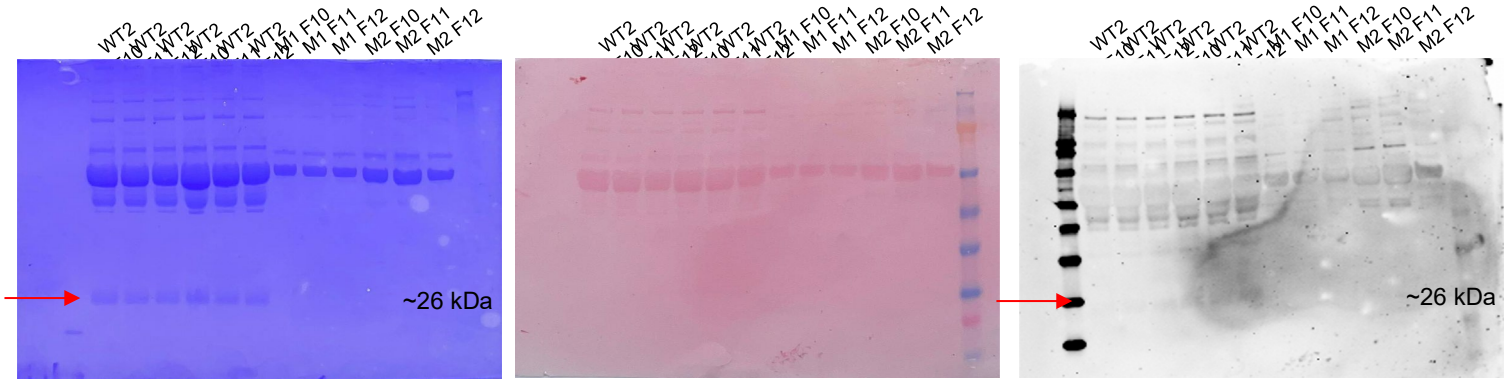

Figures 1, 2, and 3, anti-CD9 membranes. *Figure 1 (left) depicts the Coomassie Blue stain of the gel. The red arrow shows bands of interest at 26kDa. Figure 2 in the middle depicts a nitrocellulose membrane stained with Ponceau Red. Figure 3 on the right depicts the final reveal of WB, with bands of the protein of interest pointed by the red arrow; notice the darker gray stain on the right side of the membrane.*

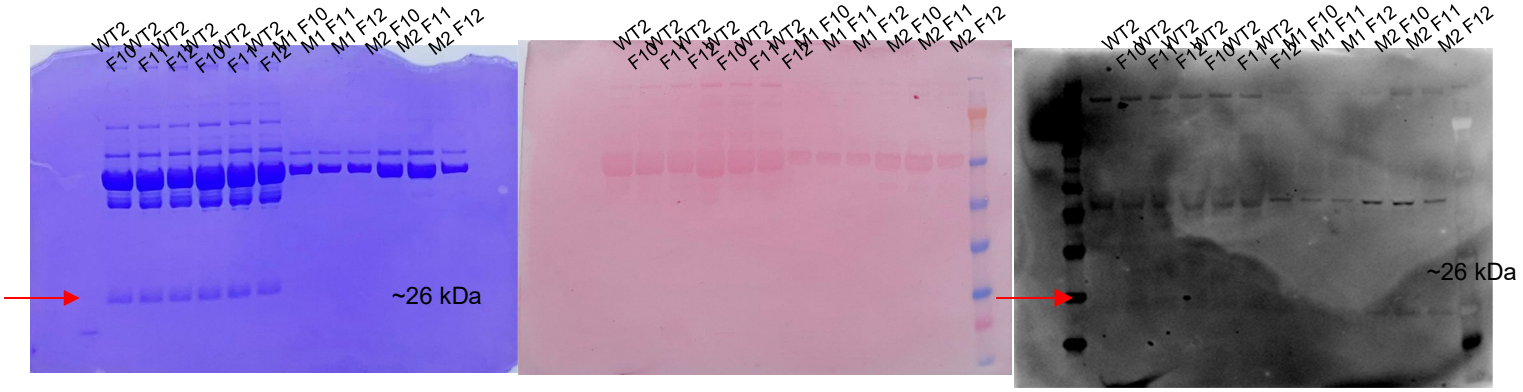

Figures 4, 5, and 6, anti-CD81 membranes. *Figure 4 (left) depicts the Coomassie Blue stain of the gel. The red arrow shows bands of interest at 26kDa. Figure 5 in the middle depicts a nitrocellulose membrane stained with Ponceau Red. Figure 6 on the right depicts the final reveal of WB, with bands of the protein of interest pointed by the red arrow; notice the lighter gray stain on the right side of the membrane.*

However, the container used to incubate antibodies on the membrane was not appropriate, yielding an unevenly stained membrane; based on membrane results, it was determined that the whole

Western Blot was to be performed again in a flat container for better results. On trial 3, the Western Blot yielded better results (Figures 7 - 12), with bands confirming the presence of exosomes. Using an even surface and utilizing PVDF membrane yielded cleaner results.

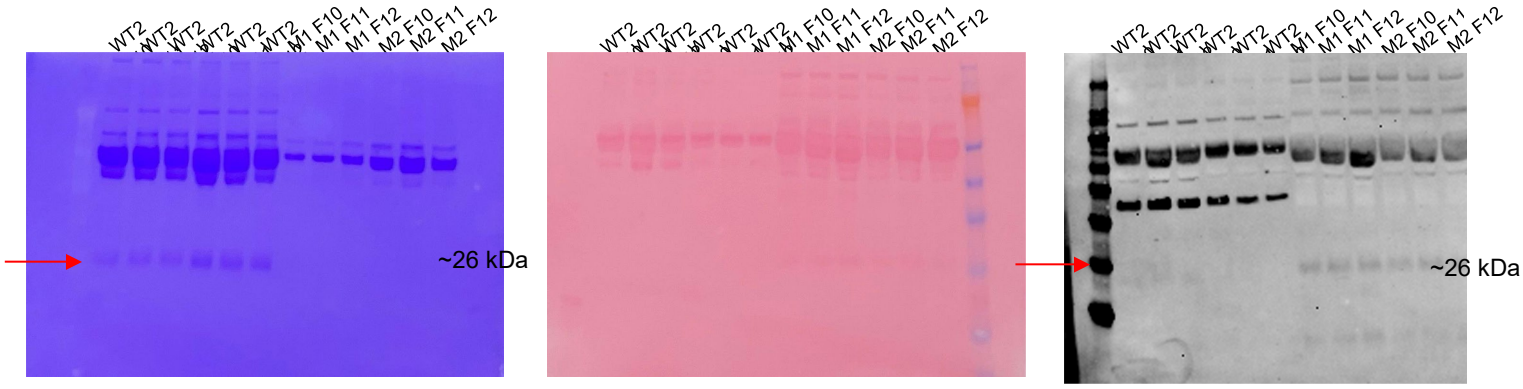

Figures 7, 8, and 9, anti-CD9 membranes. *Figure 7 (left) depicts the Coomassie Blue stain of gel. The red arrow shows bands of interest at 26kDa. Figure 8 in the middle depicts the PVDF membrane stained with Ponceau Red. Figure 9 on the right depicts the final reveal of WB, with bands of the proteins in interest pointed by the red arrow*

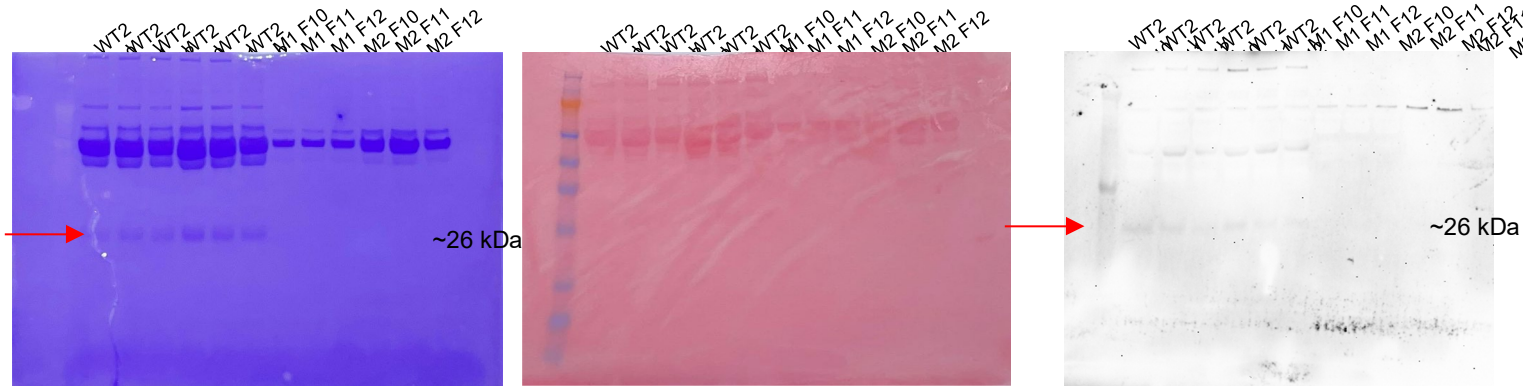

Figures 10, 11, and 12, anti-CD81 membranes. *Figure 10 (left) depicts the Coomassie Blue stain of the gel. The red arrow shows bands of interest at 26kDa. Figure 11 in the middle depicts a nitrocellulose membrane stained with*

Ponceau Red. Figure12 on the right depicts the final reveal of WB, with bands of the protein of interest pointed by the red arrow.

In the last trial, after concentrating all samples, the Western blot yielded no results due to technical and mechanical difficulties.

Discussion. From the samples obtained, we were successfully able to confirm the presence of exosomes from the plasma samples; although the results on the Western Blot seemed faint, both anti-CD9 and anti-CD81 antibodies seemed effective in proving the presence of exosomes at around the 26kDa size; however, there is still some work to be done to concentrate protein samples more effectively, and more exosome-specific antibodies to be tested. The last trial, attempted solely with the purpose of concentrating samples, proved ineffective in doing so; we hypothesize that the samples were unable to run due to the high salt content of the RIPA buffer utilized to lyse the samples. Further attempts to concentrate the samples will be done in earlier steps of the procedure, to concentrate before adding any saline buffers. Lastly, upon being able to concentrate exosomes successfully, we plan to transition to the process of isolation and to culture of cardiomyocytes in vitro, with the goal to slowly transition to exosome extraction from healthy human subjects and culturing those to pathological human heart tissue.

References

Barile, L., Lionetti, V., Cervio, E., Matteucci, M., Gherghiceanu, M., Popescu, L. M., Torre, T., Siclari, F., Moccetti, T., & Vassalli, G. (2014). Extracellular vesicles from human cardiac progenitor cells inhibit cardiomyocyte apoptosis and improve cardiac function after myocardial infarction. *Cardiovascular Research*, *103*(4), 530–541. https://doi.org/10.1093/cvr/cvu167

Barile, L., & Vassalli, G. (2017). Exosomes: Therapy delivery tools and biomarkers of diseases. *Pharmacology & Therapeutics*, *174*, 63–78. https://doi.org/10.1016/j.pharmthera.2017.02.020

EL Andaloussi, S., Mäger, I., Breakefield, X. O., & Wood, M. J. A. (2013). Extracellular vesicles: Biology and emerging therapeutic opportunities. *Nature Reviews Drug Discovery*, *12*(5), 347–357. https://doi.org/10.1038/nrd3978